

RESPONSE OF SLIDING STRUCTURES TO NEAR-FAULT PULSES: NUMERICAL AND ANALYTICAL SOLUTIONS

E. Voyagaki¹, G. Mylonakis² and I. N. Psycharis³

¹ National Technical University, Athens, Greece

^{2,3} Associate Professor, Dept. of Geotechnical Engineering, University of Patras, Greece

³ Associate Professor, Earthquake Engineering Laboratory, National Technical University, Athens, Greece

Email: eliavoyager@hotmail.com, mylo@upatras.gr, ipsych@central.ntua.gr

ABSTRACT :

Analytical and numerical solutions are presented for the plastic response of sliding structures to idealized ground acceleration pulses. These motions are typical of near-fault earthquake motions generated by forward fault-rupture directivity and may inflict large strains and displacements in the absence of substantial soil strength. The structures are modeled as rigid blocks on inclined frictional planes. Although idealized, these models are widely used by engineers for simulating a variety of systems including isolation devices, monumental structures, retaining walls, slopes, embankments and dams. Four basic simple waveforms are examined: (1) triangular; (2) sinusoidal; (3) exponential; (4) rectangular. In the first part of the article, the effect of peak strength, residual strength, and number of excitation cycles, on peak displacements is presented. Results are presented in the form of dimensionless graphs and regression formulas that elucidate the salient features of the problem. In the second part of the article, closed-form solutions are derived for plastic response and associated peak velocities and displacements. It is shown that all three time histories of ground motion (i.e., acceleration, velocity, and displacement) control peak response – contrary to the widespread view that ground velocity alone is of leading importance. The results are compared with conventional Newmark-type approaches to illustrate certain practical aspects of the solution.

KEYWORDS: near-fault, pulses, directivity, sliding systems, ground velocity, closed-form solution

1. INTRODUCTION

Following pioneering studies by seismologists and earthquake engineers in the 1970's [e.g., Boore & Zoback 1974; Bertero et al, 1978], the destructiveness of near-fault earthquake motions has become a major subject in earthquake engineering research. These motions are generated by fault-rupture directivity, as the rupture propagates towards a site (and slip vector points towards the site), located within approximately ten to twenty kilometers from fault. The resulting ground motions attain the form of high-amplitude, shock-like pulses, polarized in the strike-normal direction, concentrated in the early part of the earthquake record [Sommerville et al, 1997; Rodriguez-Marek 2000]. A number of structural failures have been attributed to near-fault pulses including those of Olive View Hospital in the 1971 San Fernando Earthquake, Elevated Hanshin Expressway in Kobe, building structures in Northridge, and a weapon industry in Greece during the 1995 Aegion earthquake. Comprehensive catalogues and models of such motions are available in the literature [Mylonakis & Voyagaki, 2006; Mavroeidis & Papageorgiou, 2003].

Most recent studies utilize actual earthquake recordings in conjunction with numerical algorithms to analyze the response of various structural and geotechnical systems to one or several ground motions [Ambraseys & Menu 1988]. On the other hand, idealized pulses that may provide useful insight in the physics of the problem have received less attention [Yegian et al 1989; Conte & Dente 1989, Mavroeidis & Papageorgiou 2003, Mylonakis & Voyagaki, 2006]. Studying simple pulses appears desirable, since there is ample evidence that only a short interval in ground motion, associated with the pulse, contributes to most of the seismic demand. In addition, simple waveforms often allow closed-form solutions to be obtained, which have distinct advantages over numerically constructed solutions.

2. PROBLEM PRESENTATION & PARAMETER DEFINITION

The problem considered in this study is that of a rigid block of mass m , resting on a rough plane of frictional coefficient μ and yielding strength Q_y , subjected to four idealized ground acceleration pulses, as shown in Figure 1. The pulses are described by their shape (rectangular, sinusoidal, triangular & exponential), amplitude A_g , half-cycle duration t_d (or, equivalently, period $T_p = 2 \times t_d$) and number of cycles (half cycle, full cycle).

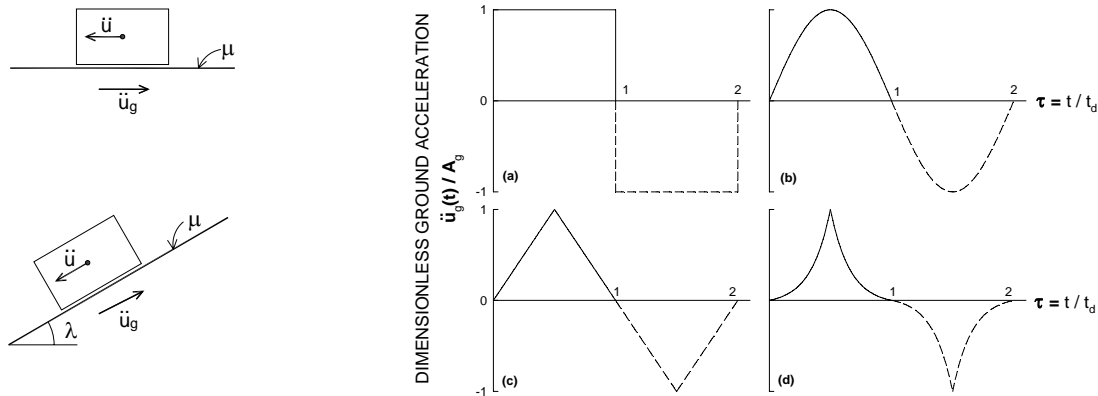


Figure 1 Sliding block and earthquake motion idealizations - Dimensionless ground acceleration time histories of four idealized ground pulses of different durations (half and full cycles): (a) rectangular; (b) sinusoidal; (c) triangular; (d) exponential.

It is well known that, from a seismological viewpoint, velocity pulses have certain advantages over acceleration pulses, as they scale better with source parameters such as moment magnitude and stress drop [Mavroeidis & Papageorgiou, 2003]. On the other hand, acceleration pulses tend to correlate better with engineering parameters such as yield seismic coefficient and inelastic displacement. This can be understood given that the triggering of plastic deformations (termed “yielding” in the ensuing) is inherently associated with acceleration – not velocity. Thereby, acceleration pulses may be equally suitable – or perhaps advantageous – over velocity pulses when plastic response is of main concern. It should also be noted that velocity and acceleration pulses are inherently interconnected, as, for instance, a full – cycle sinusoidal acceleration pulse corresponds to a half-cycle velocity pulse, a full – cycle box acceleration pulse corresponds to a half-cycle triangular velocity pulse etc.

With reference to Fig 1, both half – and full-cycle pulses are considered, denoted by solid and solid-broken lines, respectively. Strictly speaking, the former are not physically realizable, for ground velocity at the end of the excitation ($\tau = 1$) is not zero. Nevertheless, these incomplete pulses incorporate the large acceleration and velocity excursions observed in actual near-fault recordings and, thereby, are well suited for studying the main features of seismic demand imposed by such motions. In addition, it will be shown that certain sliding systems attain their peak response *before* the end of excitation and, thereby, whether ground velocity tends to zero or not at a later time becomes of less importance.

The following dimensionless quantities are used to describe the results presented below: yielding strength $\eta = Q_y/mA_g$, time of yielding $\tau_y = t_y/t_d$, time of maximum sliding $\tau_m = t_m/t_d$, where $Q_y =$ force necessary to induce sliding, $t_y =$ time of yielding, $t_m =$ time of peak displacement. In addition, peak sliding velocity V_m , maximum sliding displacement u_m , incremental ground displacement during sliding $\Delta u_g = u_g(\tau_m) - u_g(\tau_y)$, $t_{vm} =$ time of V_m , $V_g =$ peak pulse velocity, $D_g =$ peak pulse displacement, are employed in the ensuing.

3. CLOSED-FORM SOLUTIONS

3.1: Half – Cycle Pulses

The governing equation of motion of a rigid block sliding on a rough inclined plane under seismic action acting parallel to it is

$$\ddot{u} = \ddot{u}_g - \frac{Q_y}{m} \text{sgn}(\dot{u}) \quad (3.1)$$

where \ddot{u} denotes sliding acceleration relative to the inclined plane. Note that the sign in front of the seismic acceleration term \ddot{u}_g is considered positive for convenience[†].

Integrating the above equation twice with respect to time, enforcing the initial conditions of zero sliding velocity and displacement at $t = 0$, and considering unidirectional sliding in the downhill direction ($\dot{u} \geq 0$), block velocity and displacement are obtained from the closed-form expressions [Mylonakis & Voyagaki 2006]:

$$\dot{u} = \dot{u}_g - \dot{u}_g(t_y) - \frac{Q_y}{m}(t - t_y) \quad (3.2)$$

$$u = u_g - u_g(t_y) - \dot{u}_g(t_y)(t - t_y) - \frac{Q_y}{2m}(t - t_y)^2 \quad (3.3)$$

The time of peak deformation is obtained from Eqn (2) by setting block velocity equal to zero

$$t_m = t_y + \frac{m}{Q_y} [\dot{u}_g(t_m) - \dot{u}_g(t_y)] = t_y + \frac{m}{Q_y} \left(\begin{array}{l} \text{pulse area after} \\ \text{initiation of sliding} \end{array} \right) \quad (3.4)$$

which defines a motion reversal. For half-cycle pulses such as those studied in this section, it is evident that the smallest positive root of Eqn 3.4, corresponding to the *first* velocity reversal, defines the time of peak sliding. For full cycle pulses, this peak should be distinguished from peak residual response which may take place at a later time.

The above equation elucidates the intimate interconnection between pulse velocity and peak sliding displacement. Indeed, the higher the pulse area after yielding, the longer the block will stay in motion, the higher the ensuing sliding displacement. It should be kept in mind, however, that Eqns 3.1-4 tacitly assume that the block has slipped. Evidently, initiation of sliding requires considerable levels of ground acceleration and, thereby, ground velocity should not be viewed as the sole descriptor of earthquake destructiveness [Rodriguez-Marek, 2000; Mylonakis & Voyagaki 2006].

Additional support to this suggestion comes from the observation that block displacement in Eqn 3.3 depends on ground displacement u_g – not on ground velocity. Evidently, a change in ground displacement during sliding will increase or decrease block displacement without altering the restoring force. This suggests that ground displacement may be more important in design against near-fault motions than previously thought.

In terms of dimensionless time, Eqn 3.2 yields for the four half-cycle pulses in Fig 1:

$$\tau_m = \begin{cases} \frac{1}{\eta} & \text{rectangular} & (3.5a) \\ \tau_y + \frac{1}{\eta\pi}(1 + \cos \pi\tau_y) & \text{sinusoidal} & (3.5b) \\ \tau_y - \frac{1}{\eta}(\tau_y^2 - \frac{1}{2}) & \text{triangular} & (3.5c) \\ \tau_y + \frac{1}{\eta(1 - e^{-\pi})} [1 + \frac{1}{2\pi}(1 + e^{2\pi\tau_y}) - \frac{e^\pi}{\pi} - \tau_y] & \text{exponential} & (3.5d) \end{cases}$$

which correspond to the case $\tau_m \geq 1$.

[†] This is to ensure positive sliding response for positive ground acceleration. The concept is indicated with the help of the reference systems of Fig 1.

When maximum response occurs during forced sliding, $\tau_m \leq 1$, time of maximum response can be obtained from Eqn 3.4. The associated equations are rather complex and are not provided herein. Note that this case is never true for a rectangular pulse, as maximum displacement for this type of motion always occurs during free sliding. Setting t equal to t_m in Eqn 3.3 and after some straightforward algebra, the following explicit solutions are obtained for the normalized maximum displacement response:

- *Rectangular Pulse*

$$\frac{u_m}{\Delta u_g} = 1 - \eta \frac{\tau_m^2}{2\tau_m - 1} \quad (3.6a)$$

- *Sinusoidal Pulse*

$$\frac{u_m}{\Delta u_g} = 1 - \frac{\frac{\eta\pi}{2}(\tau_m - \tau_y)^2 - (\cos \pi\tau_y - 1)(\tau_m - \tau_y)}{[1 + H(\tau_m - 1)] \cdot \tau_m - \tau_y - H(\tau_m - 1) - \frac{1}{\pi} [H(\tau_m - 1) \cdot \sin \pi\tau_m - \sin \pi\tau_y]} \quad (3.6b)$$

- *Triangular Pulse*

$$\frac{u_m}{\Delta u_g} = 1 - \frac{(\tau_m - \tau_y) [\tau_y^2 + \frac{\eta}{2}(\tau_m - \tau_y)]}{1/12 - \tau_m/2 + \tau_m^2 - \tau_m^3/3 - \tau_y^3/3 - (1/3 + \tau_m^2 - \tau_m^3/3 - \tau_m) \cdot H(\tau_m - 1)} \quad (3.6c)$$

- *Exponential Pulse*

$$\frac{u_m}{\Delta u_g} = 1 - \frac{2\pi(\tau_m - \tau_y) [1 - e^{2\pi\tau_y} + 2\pi\tau_y + \eta\pi(\tau_m - \tau_y)(1 - e^\pi)]}{-e^{-2\pi(\tau_m - 1)} + e^{2\pi\tau_y} - 2\pi e^\pi (2\tau_m - 1) + 2\pi(\tau_m - \tau_y) [1 + \pi(\tau_m + \tau_y)] - [1 - e^{-2\pi(\tau_m - 1)} + 2\pi(\tau_m - 1)(\pi(\tau_m - 1) - 1)] H(\tau_m - 1)} \quad (3.6d)$$

where $H(\)$ denotes the Heaviside (step) function. In the above equations, η denotes the ratio of yielding acceleration to peak pulse acceleration [Bertero et al 1978]. In the present problem, η is related to μ , λ and A_g as

$$\eta = \frac{\tan[\text{Arc tan}(\mu) - \lambda \text{sign}(\dot{u})] g}{A_g} \quad (3.7)$$

which defines a problem of *asymmetric* friction with respect to the direction of sliding. The time of slippage is obtained from the equation:

$$\ddot{u}_g(t_y) = \frac{Q_y}{m} = \eta A_g \quad (3.8)$$

Solving Eqn 3.8 yields the following solutions for the dimensionless time τ_y

$$\tau_y = \begin{cases} 0 & \text{rectangular} & (3.9a) \end{cases}$$

$$\tau_y = \begin{cases} \frac{1}{\pi} \sin^{-1} \eta & \text{sinusoidal} & (3.9b) \end{cases}$$

$$\tau_y = \begin{cases} \frac{\eta}{2} & \text{triangular} & (3.9c) \end{cases}$$

$$\tau_y = \begin{cases} \frac{1}{2\pi} \ln[1 - \eta(1 - e^\pi)] & \text{exponential} & (3.9d) \end{cases}$$

which correspond to a rectangular, sinusoidal, triangular, and exponential pulse, respectively. The dependence of τ_y on η elucidates the sole importance of acceleration content on initiation of yielding. Note that the above displacements are both peak and residual responses due to the unilateral nature of the pulse.

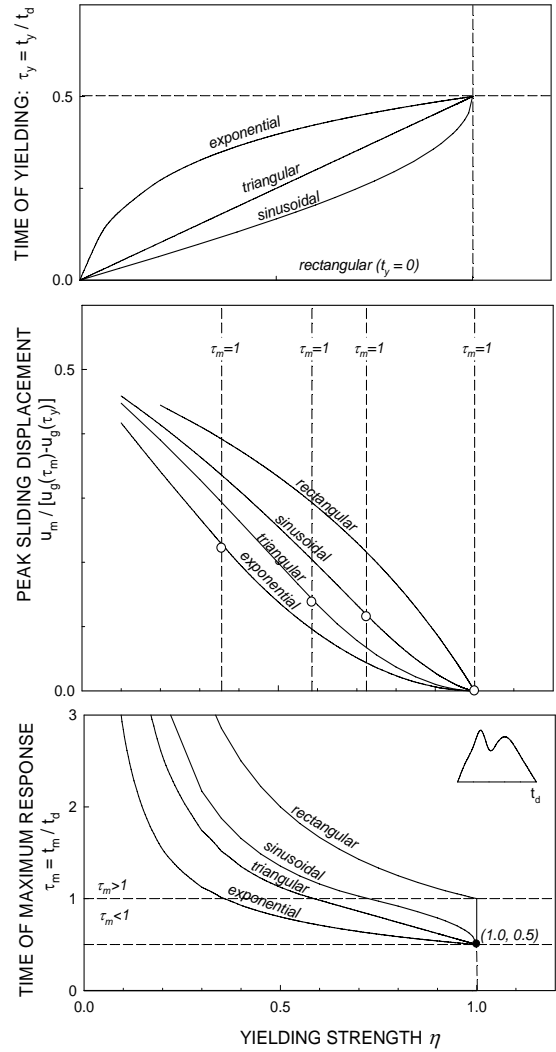


Figure 2 Normalized time of yielding, peak sliding and corresponding time as function of yielding strength for a rigid block on an inclined plane subjected unilateral sliding under four idealized half-cycle acceleration pulses.

Numerical results from Eqns 3.5 to 9 are shown in Fig 2, plotted as functions of sliding strength. Evidently, time of slippage (Fig 2a) is an increasing function of η for all pulses – except for the rectangular one, for which $\tau_y = 0$. The functional dependence of τ_y on sliding strength for the three pulses is relatively simple. As a first approximation, it can be viewed as a mere proportionality (i.e., $\tau_y \propto \eta$).

Time of maximum displacement (Fig 2c) is a decreasing function of sliding strength. The functional dependence of τ_m on η is more complex than that of τ_y . In most cases, peak displacement occurs during free sliding. Peak response during forced sliding occurs for $\eta > 0.36$ (exponential pulse), $\eta > 0.59$ (triangular pulse), and $\eta > 0.73$ (sinusoidal pulse).

Peak sliding displacement is shown in Fig 2b, plotted as fraction of incremental base displacement during sliding: $\Delta u_g = u_g(\tau_m) - u_g(\tau_y)$. This ratio is, naturally, always smaller than 1 and decreases with increasing η , reaching zero at $\eta = 1$. As pointed out by Garini & Gazetas (2007), this monotonic behavior may not be true with motions containing multiple pulses of alternating sign. Typical values lie between approximately 0.4 and 0,

implying that up to approximately 40% of incremental base displacement becomes sliding displacement. Note that the behavior close to $\eta = 0$ is anomalous (recall that block response under zero friction to a half-cycle pulse is unbounded – regardless of pulse shape), and shall not be discussed here.

3.2. Full – Cycle Pulses

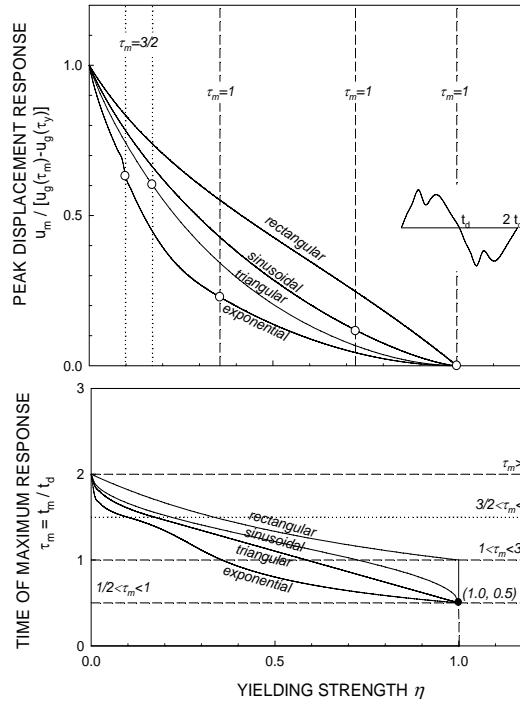


Figure 3 Normalized time of yielding, peak sliding and corresponding time as function of yielding strength for a rigid block on an inclined plane subjected unilateral sliding under four idealized full-cycle acceleration pulses.

The above analysis can be extended to the case of full-cycle pulses. For the sake of brevity, only final results are presented below. It is noted that these results assume unidirectional sliding in the downhill direction.

- *Rectangular Pulse*

$$\frac{u_m}{\Delta u_g} = 1 - \eta \frac{2}{1 - \eta(\eta - 2)} \quad (3.10a)$$

- *Sinusoidal Pulse*

$$\frac{u_m}{\Delta u_g} = 1 - \frac{\eta\pi(\tau_m - \tau_y)^2 / 2 - (\cos \pi\tau_y - 1)(\tau_m - \tau_y)}{\tau_m - \tau_y - (\sin \pi\tau_m - \sin \pi\tau_y) / \pi} \quad (3.10b)$$

- *Triangular Pulse*

$$\frac{u_m}{\Delta u_g} = 1 - \frac{12(\tau_m - \tau_y)[\tau_y^2 + \frac{\eta}{2}(\tau_m - \tau_y)]}{1 - 6\tau_m + 12\tau_m^2 - 4(\tau_m^3 - \tau_y^3) - (2\tau_m - 3)^3 H(\tau_m - 2/3)} \quad (3.10c)$$

- *Exponential Pulse*

$$\frac{u_m}{\Delta u_g} = 1 - \frac{2\pi(\tau_m - \tau_y)[1 - e^{2\pi\tau_y} + 2\pi\tau_y + \eta\pi(\tau_m - \tau_y)(1 - e^\pi)]}{\{-e^{-2\pi(\tau_m-1)} + e^{2\pi\tau_y} - 2\pi e^\pi(2\tau_m - 1) + 2\pi(\tau_m - \tau_y)[1 + \pi(\tau_m + \tau_y)]\} + [e^{-2\pi(\tau_m-1)} + e^{2\pi(\tau_m-1)} - 4\pi^2(1 - \tau_m)^2 - 2] H(\tau_m - 1) + [e^{2\pi(\tau_m-2)} - e^{-2\pi(\tau_m-1)} + 2\pi e^\pi(2\tau_m - 3)] H(\tau_m - 3/2)} \quad (3.10d)$$

where τ_m can be obtained by corresponding closed form expressions (not shown). Numerical results from equations 3.10 & 11 are presented in Figure 3, plotted as functions of η . Time of yielding for full-cycle pulses coincides with that of half-cycle pulses (Eqn 3.9). Time of maximum displacement (Fig 3b) is a decreasing function of η . The functional dependence of τ_m on η is more complex than in the previous case. In all cases, peak displacement occurs during forced sliding. Peak response during first half-cycle ($\tau_m < 1$) occurs for $\eta > 0.35$ (exponential pulse), $\eta > 0.58$ (triangular pulse), and $\eta > 0.72$ (sinusoidal pulse). For the rectangular pulse always $1 \leq \tau_m \leq 2$. Peak sliding displacement is shown in Fig 3a, normalized with incremental base displacement during sliding: Δu_g . This ratio decreases with increasing η , equal to 1 for $\eta = 0$ and reaching zero at $\eta = 1$.

4. COMPARISON WITH EXISTING SOLUTIONS

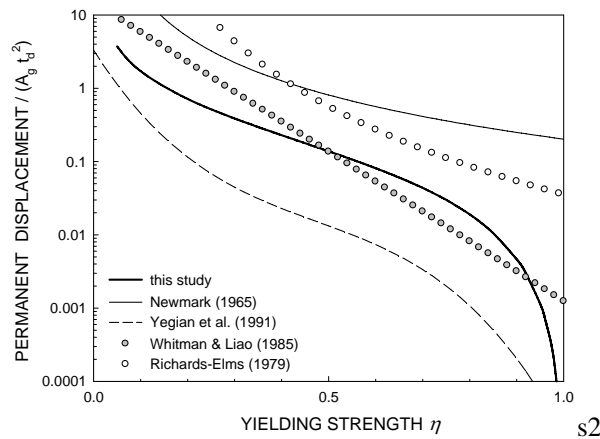


Figure 4 Comparison of permanent displacement for a half-cycle sinusoidal pulse obtained in this study, with established solutions from the literature.

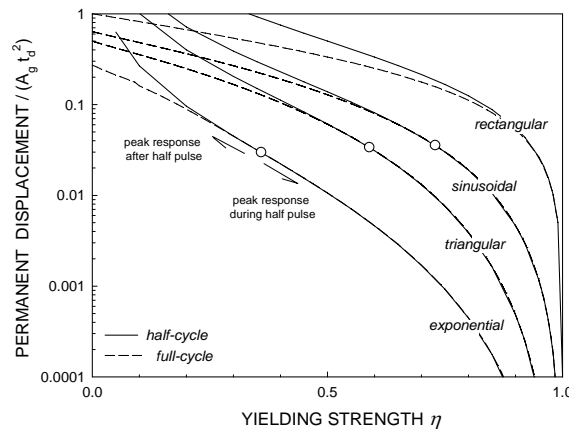


Figure 5 Comparison of permanent displacements for half and full – cycle acceleration pulses.

A comparison of permanent displacements obtained for half-cycle pulses is compared against established solutions by Newmark (1965), Richard Elms (1979), Whitman & Liao (1985) and Yegian et al (1991), in Fig 4. These solutions have been obtained for conventional (non-impulsive) motions of multiple cycles. The solutions by Newmark and Richard-Elms refer to maximum expected values, whereas those by Whitman-Liao and Yegian et al to average or median values. The herein proposed solution provides results which are comparable or higher to the median predictions – a remarkable behavior given the half cycle duration of the excitation.

A comparison of permanent displacements for half- and full-cycle pulses obtained from the herein proposed solution is shown in Fig 5. Evidently, half-cycle pulses generate more permanent displacement than their full cycle counterparts. The solutions converge with increasing yielding strength and become identical beyond $\eta = 0.36, 0.59$ and 0.73 for an exponential, triangular and sinusoidal pulse, respectively. These limiting values are identical to those shown in Fig 2 and suggest that maximum displacement is often obtained during the first half of the pulse.

5. CONCLUSIONS

The response of rigid blocks on inclined frictional planes subjected to four idealized pulses (rectangular, sinusoidal, triangular & exponential) was obtained analytically. The main conclusions of this study are:

- (1) Half-cycle pulses generate higher displacements than full – cycle pulses for equal peak acceleration, duration and frictional strength. This is in contrast to ordinary (non impulsive) motions, for which displacement increases with increasing cycles.
- (2) Permanent displacements for the herein-studied idealized pulses are comparable or higher to mean values obtained by established solutions in the literature. This is remarkable given the limited duration of the idealized motions, and elucidates the fundamental differences between plastic response to ordinary and impulsive ground motions.
- (3) The highly complex dependence of peak displacement with frictional strength η is elucidated in equations (6) and (10). This suggests that simple scaling laws of power or exponential nature may not be possible – even for simple pulses such as those studied in this paper.

REFERENCES

- Ambraseys NN, Menu JM (1988). Earthquake-Induced Ground Displacements. *Earthquake Engineering and Structural Dynamics* **16**, 985-1006
- Bertero VV, Mahin SA, Herrera RA (1978). Aseismic design implications of near-fault San Fernando earthquake records. *Earthquake Engineering and Structural Dynamics* **6**, 31-42
- Boore DM, Zoback MD (1974). Near-field motions from kinematic models of propagating faults. *Bulletin of the Seismological Society of America* **64**, 321-342.
- Conte E, Dente G (1989). An Analytical Solution for Newmark's Sliding Block. *Soils & Foundations* **29:3**, 152-156
- Garini E, Gazetas G (2007). Sliding of Rigid Block on Sloping Plane: The Surprising Role of the Sequence of Long-Duration Pulses. *Proc. 2nd Japan-Greece Workshop on Seismic Design, Observation, & Retrofit of Foundations*, April 3~4, Tokyo, Japan
- Mavroeidis G, Papageorgiou A (2003). A mathematical representation of near-fault ground motions. *BSSA* **93:3**, 1099-1131
- Mylonakis G, Voyagaki E (2006). Yielding Oscillator subjected to simple pulse waveforms: numerical analysis & closed-form solutions. *Earthquake Engineering and Structural Dynamics* **35**, 1949-1974
- Rodriguez-Marek A (2000). *Near-fault seismic site response*. Ph.D. Dissertation, Department of Civil Engineering, University of California, Berkeley
- Somerville PG, Smith NF, Graves RW, Abrahamson NA (1997). Modification of empirical strong motion attenuation relations to include amplitude & duration effects of rupture directivity. *Seism. Res Lett* **68**, 199-222
- Yegian MK, Marciano EA, Gharaman VG (1991) Earthquake-induced permanent deformations: probabilistic approach. *Journal of Geotechnical Engineering, ASCE* **117:1**, 35-50